SIMULATING A HEXAPHONIC PICKUP USING PARALLEL COMB FILTERS FOR GUITAR DISTORTION

Sebastian Laguerre and Gary P. Scavone

Computational Acoustic Modeling Laboratory (CAML)
Centre for Interdisciplinary Research in Music Media and Technology (CIRMMT)
Schulich School of Music, McGill University, Montréal, Canada
sebastian.laguerre@mail.mcgill.ca | gary.scavone@mcgill.ca

ABSTRACT

This paper introduces hexaphonic distortion as a way of achieving harmonically rich guitar distortion while minimizing intermodulation products regardless of playing style. The simulated hexaphonic distortion effect described in this paper attempts to reproduce the characteristics of hexaphonic distortion for use with ordinary electric guitars with mono pickups. The proposed approach uses a parallel comb filter structure that separates a mono guitar signal into its harmonic components. This simulates the six individual string signals obtained from a hexaphonic pickup. Each of the signals are then individually distorted with oversampling used to avoid aliasing artifacts. Starting with the baseline of the distorted mono signal, the simulated distortion produces fewer intermodulation products with a result approaching that of hexaphonic distortion.

1. INTRODUCTION

Distortion effects have been around since the inception of the electric guitar. They add sustain and harmonic overtones to create a richer, warmer sound. The distorted sounds that characterize many rock genres are the result of a non-linear process that produces frequencies not present in the original signal. When the input signal comprises a single sinusoidal frequency, the output of a non-linear system will contain integer multiples of the input frequency. However, if multiple frequencies are present in the input, the output of the system will also contain intermodulation products that may not be harmonically related to each other [1]. The resulting spectrum can be so dense that it can sound harsh and undefined. While useful for many music genres, it is not always what is desired.

1.1. Motivation

This research comes at the request of a musician who wished to recreate the hexaphonic distortion effects used by the Brazilian psychedelic rock group, Os Mutantes. Since a hexaphonic pickup was unavailable to the musician and likewise for many others, it became of interest to research a method by which hexaphonic distortion could be simulated through digital signal processing techniques, allowing guitarists with regular mono pickups to achieve this iconic sound.

Copyright: © 2021 Sebastian Laguerre et al. This is an open-access article distributed under the terms of the Creative Commons Attribution 3.0 Unported License, which permits unrestricted use, distribution, and reproduction in any medium, provided the original author and source are credited.

2. BACKGROUND

In any guitar pickup, vibrations in the strings are converted to an electrical signal that is then amplified. The output of a standard mono guitar pickup is the combined signal of all six strings. Because of this, guitarists will sometimes limit their use of distortion to single notes or power chords consisting of fifths and octave intervals to prevent the sound from becoming muddled.

2.1. Hexaphonic Distortion

The Os Mutantes secret to avoiding intermodulation was to use an independent pickup for each string and one distorter for each pickup, for a total of six fuzz distorters per guitar [2]. A hexaphonic pickup, as it is commonly known, provides individual signals for each string. Distorting these signals separately results in fewer intermodulation products while retaining the harmonic enrichment.

The hexaphonic pickup has many uses beyond distortion. It found its most widespread use in guitar synthesizers. Early guitar synthesizers such as the EMS Synthi Hi-Fli (1973) were nothing more than multi-effects processors without actual synthesis circuitry. The late 1970s saw the introduction of three guitar synthesizers; the ARP Avatar, the 360 Systems Spectre, and notably, the Roland GR-500 [3]. Unlike earlier guitar synthesizers, these three comprised a controller guitar fitted with a hexaphonic pickup and a separate polyphonic synthesizer module connected by a multiconductor patch cable. While the ARP Avatar and the Spectre were commercial failures, the GR-500 was well received and Roland went on to develop a variety of guitar synthesizer products.

There are numerous other companies now offering hexaphonic guitars and aftermarket conversion kits. Hexaphonic distortion effects have occasionally appeared on the market, such as the Roland GR-100, and most recently, the Spicetone 6Appeal [4]. Unfortunately, these effects all require an expensive hexaphonic pickup guitar and for this reason hexaphonic effects have remained niche.

2.2. Reducing Intermodulation Distortion

While there is much literature on digital distortion effects, the role of intermodulation is not often addressed and only a few algorithms attempt to minimize intermodulation distortion in their design. Such approaches are based on multiband distortion units, the most popular of which is the Quadrafuzz [5]. By splitting the input signal into separate frequency bands and applying a clipping distortion to each band independently, multiband distortion limits the intermodulation components to those in a given band.

Fernández-Cid and Casajús Quirós [6] took this concept to the extreme, combining a waveshaping function with a 13-band filter

bank. Their research was focused on achieving a highly customizable type of distortion through the use of Chebyshev polynomials that offer precise control over the harmonic partials. Timoney et al. [7] furthered this concept by showing that static waveshaping could be used to emulate analog distortion circuits. Abel and Werner [8] applied this technique to a modal reverberator architecture to produce distortion without intermodulation products.

However, no one has yet explored a method to simulate hexaphonic distortion. Guitar pickups exhibit their own non-linear behaviour [9]. With the addition of cross-talk between individual pickups and sympathetic vibrations [10], the individual signals of a hexaphonic pickup will always contain some unrelated harmonics. When distorted, these introduce limited amounts of intermodulation thereby giving hexaphonic distortion its distinctive tone.

2.3. Harmonic Sound Separation

Many instruments, including the guitar, produce predominantly harmonic sounds that consist of integer multiples of a fundamental frequency f_1. A comb filter also exhibits peaks at integer multiples of a fundamental frequency and can therefore be used to reduce harmonic interference or to enhance a harmonic signal buried in noise, provided the "teeth" of the comb coincide with the harmonics of the signal.

Välimäki et al. [11] demonstrated several such approaches. A comb filter is used to attenuate the harmonic components of a signal thereby extracting the background noise component. By cascading the comb filter with a 2nd-order resonance filter, it is possible to extract a single harmonic component.

When used in parallel, comb filters can separate harmonic signals. A comb filter with peaks located at the multiples of the second harmonic f_2 will extract even harmonics and a complementary comb filter with peaks shifted by $f_2/2$ will extract odd harmonics. This method is used in digital color TV systems to separate the interlaced luminance and chrominance signals in composite video signals [12].

Comb filters have been employed in sound source separation and polyphonic pitch detection, where the application is automatic music transcription. Miwa et al. [13] developed a method of detecting the pitch of music played by several instruments by observing the intermediate outputs of a series combination of twelve comb filters each attenuating a tone from C to B.

Gainza et al. [14] revisited the use of comb filters for musical sound source separation, this time relying on multi-pitch estimation (MPE) to detect the comprising signal pitches, followed by frequency-domain filtering.

In classical waveform synthesis, the sampling of continuous-time waveforms with frequencies above the Nyquist limit introduces aliasing distortions. J. Pekonen and V. Välimäki [15] proposed a combination of IIR comb filter and DC blocking filter to attenuate aliasing distortions that lie between the harmonics.

3. HEXAPHONIC PICKUP RECORDINGS

The recordings of an actual hexaphonic pickup provided vital insights into hexaphonic audio signal characteristics and later served as the reference in the evaluation of the simulated hexaphonic distortion.

The Ubertar Hex Plus hexaphonic pickup [16] takes the shape of a single coil pickup but consists of six low-noise HC coils. The breakout box provides ¼" outputs for each string. These were connected to the high impedance instrument inputs of an RME Micstasy 8-channel preamplifier and A/D converter. The mono neck pickup was simultaneously recorded on the seventh channel.

Plucking each string with a capo at each fret position creates a complete set of recordings covering the entire chromatic scale over three octaves from E_2 to E_5. As an example, Fig. 1 shows the six-channel hexaphonic pickup recording and Fig. 2 the mono neck pickup recording of the open strings.

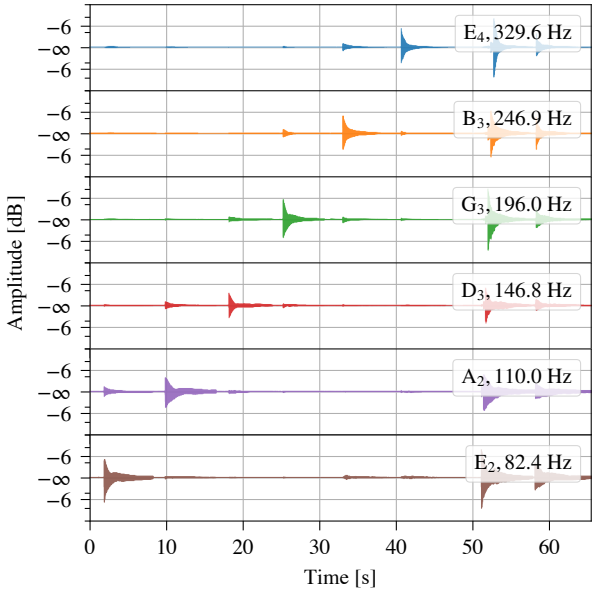

Figure 1: *Open strings hexaphonic pickup recording. There is a small amount of signal cross-talk (bleed) to adjacent pickups. The presence of a signal in the low* E_2 *pickup when plucking high* E_4 *is due to sympathetic vibrations.*

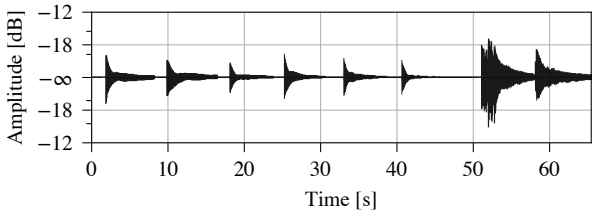

Figure 2: *Open strings mono pickup recording. Plucks of low* E_2 *to high* E_4 *followed by two strums.*

Vibrating strings generally exhibit harmonic spectral content. In the case of the electric guitar, a single guitar tone consists of frequency components at a fundamental plus all odd and even harmonics with magnitudes of the higher partials diminishing as the frequency increases [1]. This intrinsic characteristic of plucked strings is made evident by the strong presence of harmonics in the individual pickup signals. As seen in Fig. 3, the separate outputs of the hexaphonic pickup are predominantly harmonic with a magnitude response resembling the teeth of a comb filter.

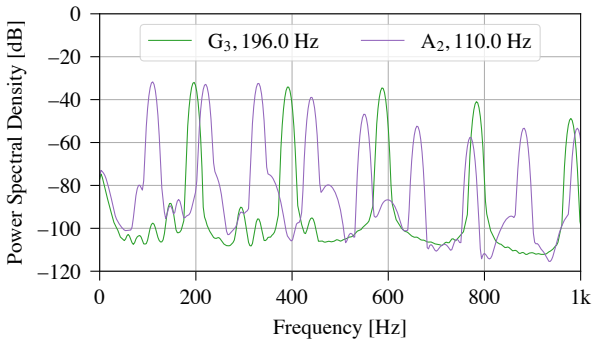

Figure 3: *Magnitude spectrum of plucked open* A_2 *and* G_3 *strings recorded using a hexaphonic pickup.*

4. SEPARATION OF HARMONIC SIGNALS

Frequency analysis of the hexaphonic pickup signals inspired a parallel comb filtering structure that separates a mono signal into harmonically related signals for subsequent effect processing. This section describes the harmonic signal separation algorithm by introducing several digital signal processing concepts and discussing their implementation in the system.

4.1. FIR Comb Filter

The finite impulse response (FIR) feedforward comb filter is obtained by summing an input signal with the same signal delayed by M samples. The difference equation of the feedforward comb filter is given by

$$y[n] = b_0 x[n] + b_M x[n - M], \tag{1}$$

where $x[n]$ is the input signal and $y[n]$ is the output signal. b_M is the feedforward gain coefficient and b_0 is the blend coefficient.

The transfer function relates the Z-transforms of input signal and output signal of the described system,

$$H_{\mathrm{FF}}(z) = \frac{Y(z)}{X(z)} = b_0 + b_M z^{-M}. \tag{2}$$

The feedforward comb filter has spectral peaks at frequencies that are multiples of $2\pi/M$ for positive values of b_M and nulls at multiples of $2\pi/M$ for negative values of b_M. In other words, changing the sign of b_M results in a comb filter with peaks shifted by π/M. To extract a harmonic signal, the peaks must coincide with the integer multiple harmonics so only positive coefficients are of interest.

For a normalized magnitude response between 0 and 1, the transfer function becomes [11]

$$H(z) = \frac{1}{2}(1 + z^{-M}). \tag{3}$$

The 3-dB width $\Delta\omega$ of the comb filter is defined as the width of the peaks at half the maximum of the magnitude squared response. The 3-dB width of the peaks of the FIR comb filter is $\Delta\omega = \pi/M$. This corresponds to the maximum possible peak width, equal to the separation between peaks at the 3-dB level.

4.2. IIR Comb Filter

The infinite impulse response (IIR) feedback comb filter is obtained by summing an input signal with a delayed version of the output attenuated by a feedback gain a_M. This produces a magnitude response with the appearance of a comb where a larger gain factor produces sharper peaks. The feedback comb filter has the difference equation

$$y[n] = x[n] + a_M y[n - M]. \tag{4}$$

The corresponding transfer function is given by

$$H_{\mathrm{FB}}(z) = \frac{1}{1 - a_M z^{-M}}. \tag{5}$$

In a similar fashion to the feedforward comb filter, the feedback comb filter has peaks at frequencies that are multiples of $2\pi/M$ for positive values of a_M and nulls at multiples of $2\pi/M$ for negative values of a_M.

The magnitude response has a minimum of $1/(1 + a_M)$ at the nulls and a maximum of $1/(1 - a_M)$ at the peaks, with $|a_M| < 1$ required for stability. Unlike with the FIR comb filter, a null magnitude of 0 is unattainable. However, the IIR comb filter has an adjustable peak width $\Delta\omega$ better suited to the separation of harmonic signals.

The ideal comb filter for harmonic separation would offer both an adjustable peak width and a normalized magnitude response with null values of 0 corresponding to a $-\infty$ dB attenuation between harmonic frequencies. This filter is achieved in the form of the universal comb filter constructed from the combination of the FIR and IIR comb filters [1].

4.3. Universal Comb Filter

The series combination of the feedforward (2) and feedback (5) comb filters leads to the universal comb filter with a new response given in the frequency-domain as

$$H_{\mathrm{UNI}}(z) = H_{\mathrm{FF}}(z) H_{\mathrm{FB}}(z) = \frac{b_0 + b_M z^{-M}}{1 - a_M z^{-M}}. \tag{6}$$

The direct-form I difference equation of the universal comb filter is given by

$$y[n] = b_0 x[n] + b_M x[n - M] + a_M y[n - M]. \tag{7}$$

This implementation requires two delay lines. Alternatively, the canonical implementation shown in Fig. 4 requires a single delay line and is described by the difference equations

$$\begin{aligned} x_h[n] &= x[n] + a_M x_h[n - M] \\ y[n] &= b_0 x_h[n] + b_M x_h[n - M]. \end{aligned} \tag{8}$$

In the special case where $b_0 = -a_M$ and $b_M = 1$, this filter structure reverts to a first-order allpass filter used in Schroeder reverberators [17].

4.4. Parameters

The delay of the filter M is fixed according to the fundamental frequency of interest. To extract frequencies that are multiples of f_1 the length of the delay line is set to

$$M = \frac{2\pi}{\omega_1} = \frac{f_s}{f_1} \quad \text{where} \quad \omega_1 = \frac{2\pi f_1}{f_s}. \tag{9}$$

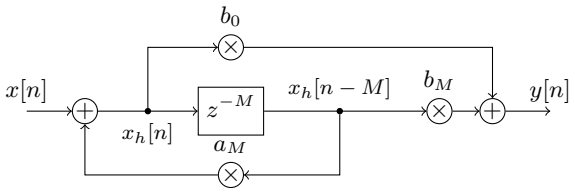

Figure 4: *The canonical universal comb filter.*

The coefficients are chosen such that the peaks of the comb filter are normalized for unity-gain:

$$a_M = \frac{1-\beta}{1+\beta}, \quad b_0 = b_M = \frac{\beta}{1+\beta}, \tag{10}$$

where

$$\beta = \tan\left(\frac{M\Delta\omega}{4}\right), \tag{11}$$

for a desired 3-dB width $\Delta\omega$ in the range $0 \leq \Delta\omega \leq \pi/M$. This maximum $\Delta\omega$ occurs when the peak width is equal to the separation between peaks at the 3-dB level. This limit applies the following constraints on β and a_M:

$$0 \leq \beta \leq 1, \quad 0 \leq a_M \leq 1. \tag{12}$$

Figure 5 shows the comb filter frequency response for different 3-dB widths.

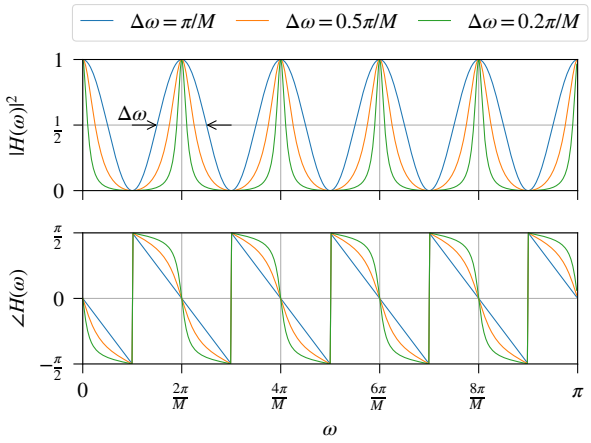

Figure 5: *The magnitude squared and phase responses for different choices of $\Delta\omega$ where $M = 10$.*

The corresponding quality factor is given by

$$Q = \frac{\omega_1}{\Delta\omega} = \frac{2\pi/M}{\Delta\omega}, \tag{13}$$

such that a narrower peak results in a higher Q. An equivalent expression for β is

$$\beta = \tan\left(\frac{\pi}{2Q}\right). \tag{14}$$

where $Q \geq 2$.

4.5. Impulse Response

The filtering operation results in an inherent temporal smearing of the signal that has the effect of smoothing out sharp transitions. The amount of temporal smearing is dictated by the filter impulse response. The universal comb filter has the causal impulse response, found by inverse Z-transform of the transfer function by partial fraction expansion,

$$h[n] = b_0\delta[n] + (a_M b_0 + b_M)\sum_{k=0}^{\infty} a_M^k \delta[n - kM - M]. \tag{15}$$

After sample M, the impulse response of a pole-zero filter with M zeros behaves like that of an all-pole filter [12]. Since M is fixed, the a_M coefficient solely defines the impulse response decay time for a given sampling frequency. The decay time is typically represented by the t_{60} measure, defined as the time for the impulse response to decay by 60 dB. Given the definition in (10) and the constraints of (12), it can be observed that the maximum amplitude of the impulse response occurs not at $n = 0$ but rather $n = M$:

$$h[M] = a_M b_0 + b_M = a_M b_0 + b_0, \tag{16}$$

which is greater than $h[0] = b_0$. This is illustrated in Fig. 6. By considering the start of the decay at $n = M$, the decay time is

$$t_{60} = \frac{M}{f_s}\left(\frac{-3}{\log a_M} + 1\right). \tag{17}$$

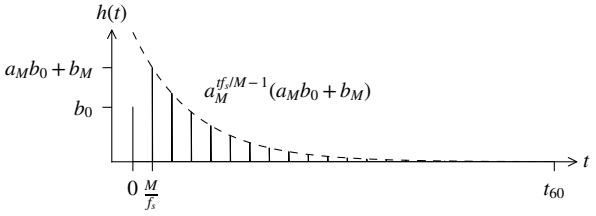

Figure 6: *Typical impulse response of the comb filter with $h[0]$, $h[M]$, and t_{60} annotated. The dashed line shows the exponential decay function.*

Using the definition in equation (14), the a_M coefficient can be expressed as

$$a_M = \frac{1 - \tan(\pi/2Q)}{1 + \tan(\pi/2Q)}. \tag{18}$$

With the addition of definition (9), equation (17) can be expressed solely in terms of f_1 and Q factor:

$$t_{60} = \frac{1}{f_1}\left(\frac{-3}{\log\left(\frac{1-\tan(\pi/2Q)}{1+\tan(\pi/2Q)}\right)} + 1\right). \tag{19}$$

This relationship between f_1, Q, and t_{60} is illustrated in Fig. 7.

The pluck or attack part of a guitar note is severely attenuated for a very long decay time t_{60}. The individual onsets get blurred together when played in fast succession. At the same time, a higher Q results in a smaller peak width and is more effective in attenuating neighbouring frequencies. This creates a trade-off between harmonic separation and sharp transitions. In the implementation, this is left as a user-adjustable parameter.

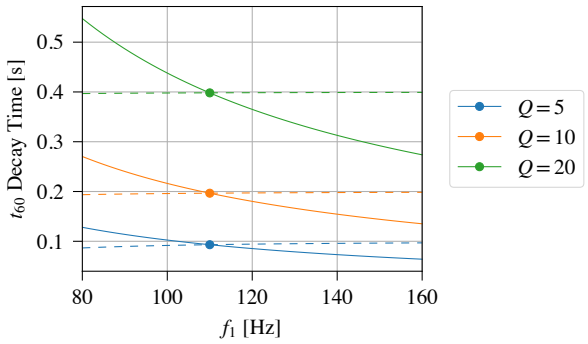

Figure 7: *Three choices of Q are plotted with their corresponding t_{60} decay time for the frequency 110 Hz. t_{60} values are extended for constant Q (solid line) and constant $\Delta\omega$ (dashed line).*

5. PARALLEL COMB FILTERS

The separation of a mono signal into harmonic signals is illustrated in the comparison of the original six-channel hexaphonic recording in Fig. 1, the mono recording in Fig. 2, and the six channels extracted from the mono signal in Fig. 8. The parallel comb filters recover each of the individual string plucks by separating each tone.

5.1. Simulating Sympathetic String Effects

As seen in Fig. 1, the hexaphonic pickup exhibits small amounts of cross-talk in which an individual pickup will capture the vibrations of an adjacent string. In addition to cross-talk, strings that are not directly interacted with also resonate due to sympathetic vibrations. Interestingly, the parallel filter bank exhibits a characteristic analogous to the sympathetic vibrations captured by a hexaphonic pickup. For example, as seen in Fig. 8, the comb filter with fundamental frequency 82.4 Hz has peaks that capture the partials of the B_3 string (246.9 Hz) and also those of the high E_4 string (329.6 Hz). In effect, it recaptures some of the sympathetic vibration signals found in hexaphonic recordings.

5.2. Filter Bank

Guitar fundamental frequencies range from 82.4 Hz to a little over 1 kHz with the upper limit depending on the number of frets. A filter bank of twelve comb filters is sufficient to separate all harmonics belonging to the musical notes in the equal temperament tuning of the fretboard. The fundamental frequencies of these filters are set to the chromatic progression of the low E string. Higher octaves of a given fundamental frequency are captured in the higher harmonic peaks. With inspiration from Miwa et al. [13], the ith harmonic of tone p is notated $f_{i,p}$, with each harmonic being a multiple of the fundamental frequency,

$$f_{i,p} = i f_{1,p}, \quad p = \mathrm{E}, \mathrm{F}, \ldots, \mathrm{D}^\sharp. \tag{20}$$

The magnitude response of the filter bank is shown in Fig. 9. Notes separated by consonant intervals will have overlapping harmonic peaks.

The comb filter transfer function with peaks at the harmonics of tone p is denoted $H_p(z)$. Without the use of oversampling, the rounding error caused by an integer sample delay, with a sample rate of 44.1 kHz, is at most 0.17%. However, with 16× oversampling, which is necessary for the distortion processing to be discussed in Sec. 6.1, the rounding error is reduced to 0.01% in the worst case, avoiding the need for fractional delay line methods.

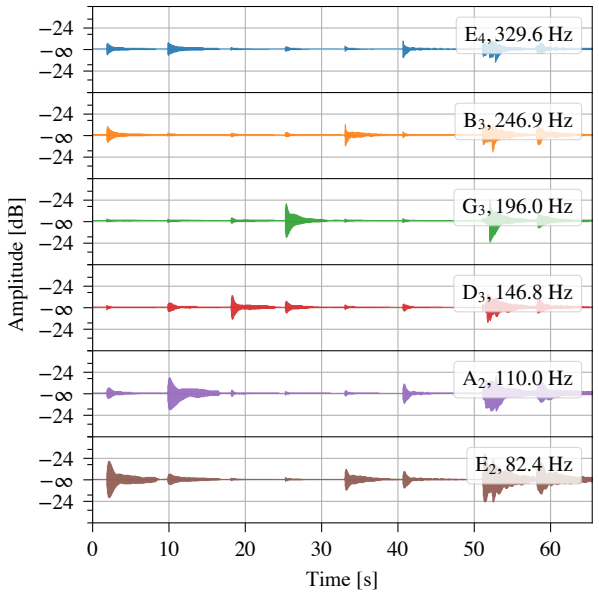

Figure 8: *Output signals of six comb filters with peaks aligned to the harmonics of the open string frequencies. Input signal is the mono pickup recording. Where the peaks of the comb filters overlap, the harmonics of the tones appear at the output of multiple comb filters.*

The combined transfer function of the filter bank is obtained by summing the frequency response of the parallel filters,

$$H_{\mathrm{sum}}(z) = \sum_p H_p(z) = H_{\mathrm{E}}(z) + H_{\mathrm{F}}(z) + \cdots + H_{\mathrm{D}^\sharp}(z). \tag{21}$$

The combined magnitude response, $|H_{\mathrm{sum}}(z)|$, is shown in Fig. 10 for different Q factors.

The first null of each comb filter combine to create a large single null at 55.4 Hz. With a high Q factor, the overlapping harmonic peaks and nulls of the parallel filters create an irregular magnitude response at high frequencies. A smaller Q factor minimizes the irregularities but is less effective at separating the signal into harmonic components. A good compromise exists at $Q = 10$ or $\Delta\omega = 0.2\pi/M$, where the magnitude response is nearly linear in the range $f_{1,\mathrm{E}}$ = 82.4 Hz to $f_{1,\mathrm{D}^\sharp}$ = 155.6 Hz.

The parallel filters can be designed with either a constant Q factor or a constant $\Delta\omega$. When the comb filters have constant Q, as shown here, the peak width increases with f_1, which makes the summed magnitude response of the parallel comb filter bank flatter. On the other hand, as was in seen Fig. 7, the impulse response decay times t_{60} vary widely over the frequencies that make up the filter bank. For this reason, a constant $\Delta\omega$, which provides nearly constant t_{60} across the filter bank frequencies, may be preferred.

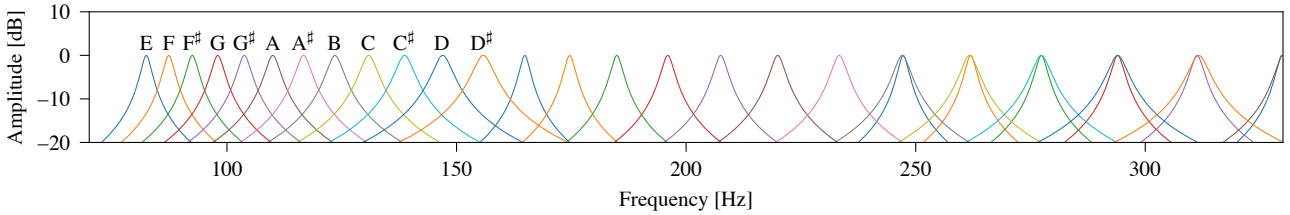

Figure 9: *Magnitude response of the twelve parallel comb filters where* $\omega = 0.05\pi/M$. *Annotated are the* $f_{1,p}$ *fundamental frequencies. Overlapping peaks occur at the coincident partials, e.g.* $f_{2,\mathrm{B}} = 246.9$ *Hz and* $f_{3,\mathrm{E}} = 247.2$ *Hz.*

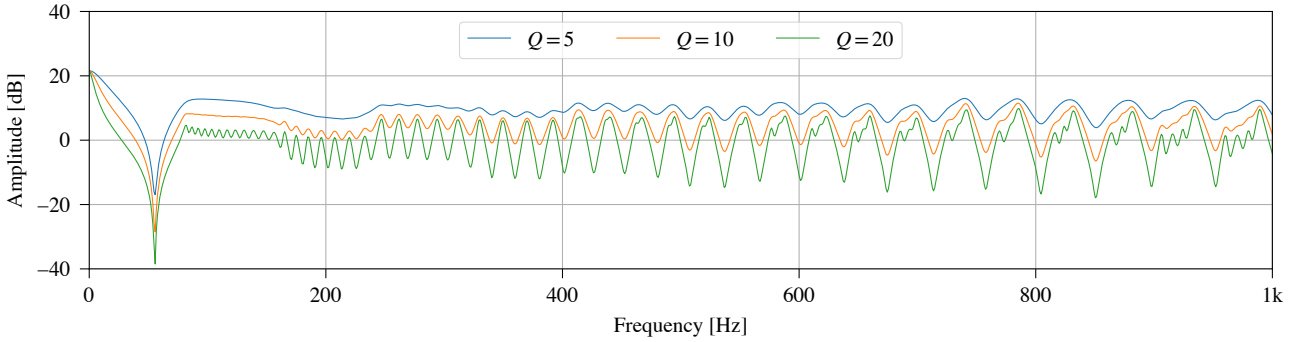

Figure 10: *Summed magnitude response of the parallel comb filters for different Q factors. Overlapping harmonic peaks and nulls of the parallel filters result in an irregular magnitude response at high frequencies.*

5.3. Microtonal Pitch Variations

Since the peaks of the filter bank are tuned to a chromatic scale, pitches that lie between semitones are attenuated. The magnitude response of Fig. 10 provides some insight into the behaviour of the filter during string bending, slides, or the use of a whammy bar. These playing techniques are all forms of glissandi — a continuous frequency increase or decrease from one note to another. As the pitch slides across harmonic peaks, it experiences amplitude modulations with an envelope resembling that of the magnitude response. This is yet another tradeoff in the choice of peak width and a further motivation for making the parameter user-adjustable.

6. EVALUATION

The simulated hexaphonic distortion effect is compared to mono and real hexaphonic distortion with regards to intermodulation products. The type of pickup and pickup position used on an electric guitar will result in very different tones. This makes comparisons difficult between the real hexaphonic distortion and the simulated effect when applied to a mono pickup. For this reason, the subsequent analyses and comparisons make use of a mono signal created by averaging the individual signals of the hexaphonic pickup.

6.1. Distortion

The non-linear clipping function [1] used in the evaluation of the simulated hexaphonic distortion is given by

$$f(x) = \mathrm{sgn}(x)(1 - e^{-|gx|}), \tag{22}$$

where g is the distortion gain. This symmetrical soft clipping produces only odd harmonics. It is chosen for its computational simplicity and predictable behaviour.

A well documented artifact of digital distortion is aliasing, whereby the harmonics produced by the non-linear effect extend beyond the Nyquist limit and wrap around to harmonically unrelated frequencies [1]. To accurately evaluate the spectral characteristics of the effect, the distortion must not introduce any aliased frequencies which would confound the analysis. Alias-free distortion is achieved by the use of sixteen-times oversampling using the popular `r8brain-free-src` library [18].

6.2. Comparison of Distortion Structures

In Fig. 11, the mono signal is distorted by the clipping function, $f(x)$. In the simulated distortion structure of Fig. 12, the same mono signal is separated into harmonic signals by the parallel comb filter bank prior to distortion. The comb filters are set to constant peak width of $\Delta\omega = 0.0015/16$ corresponding to a geometric mean Q of 10.75. In hexaphonic distortion, the clipping function is applied to each string separately, as shown in Fig. 13. In each case, the distortion gain is 100.0 and the post-distortion output signal is normalized to the root mean square (RMS) value of -12 dB. Oversampling is employed throughout each structure.

6.3. Magnitude Response Comparison

To best demonstrate the ability of the effect to reduce intermodulation distortions, recordings of the individual plucks of the open strings are combined to create pairs of varying note intervals.

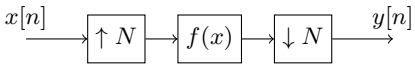

Figure 11: *The mono distortion structure.*

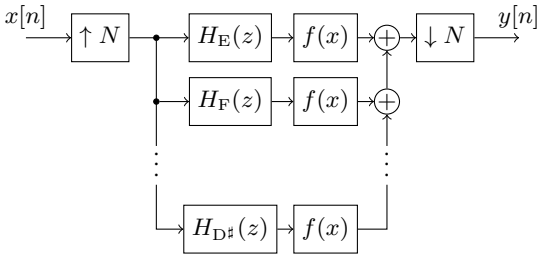

Figure 12: *The simulated distortion structure.*

Consider the minor seventh interval consisting of the tones G_3 (196 Hz) and A_2 (110 Hz). Shown in Fig. 14, when mono distortion is applied to the averaged hexaphonic signal, the three largest intermodulation products have the sum and difference frequencies given in Table 1. The difference between the peak amplitude at 110 Hz and each of these intermodulation components is shown for each distortion effect. On average, the comb filtering method in the simulated distortion attenuates the intermodulation products seen in the mono distortion by 11.6 dB, while hexaphonic distortion achieves 34.4 dB. This suggests the algorithm is about a third as effective at reducing intermodulation distortion in this particular note pair when compared to hexaphonic distortion.

Table 1: *Comparison of intermodulation product magnitudes for note pair* G_3–A_2

Intermodulation component [Hz]	306	416	636
Mono distortion [dB]	−18.3	−18.3	−19.8
Simulated distortion [dB]	−26.0	−31.2	−34.1
Hexaphonic distortion [dB]	−50.7	−54.4	−54.6

6.4. Spectrogram and Sound Comparisons

Figure 15 shows spectrograms for each distorted pairwise note combinations of the open string notes for frequencies up to 1 kHz. The double octave interval E_4–E_2 shows no intermodulation products in any of the distortion outputs. Conversely, the interval G_3–A_2 has few coincident partials. The resulting spectrogram of the mono distortion output is very dense. In the simulated distortion, the intermodulation products are partly attenuated. The reader is encouraged to compare the sound files available online [19]. For example, there is a discernible buzz in the mono-distorted E_4–D_3 interval which is not present in the other two. In the interval B_3–G_3, the mono distortion quickly decays into a noisy, dull, and undefined sound. In the simulated and hexaphonic distortion outputs, the harmonics are prominant and sustained for the entire duration.

6.5. Algorithm Performance

The filter bank and distortion structures were implemented using the Synthesis ToolKit in C++ (STK) [20]. The algorithm process

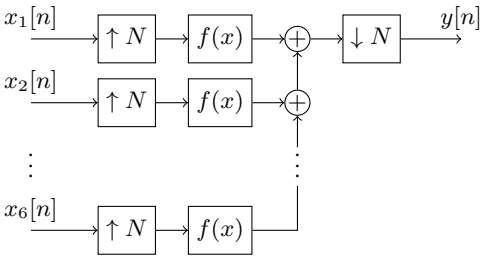

Figure 13: *The hexaphonic distortion structure.*

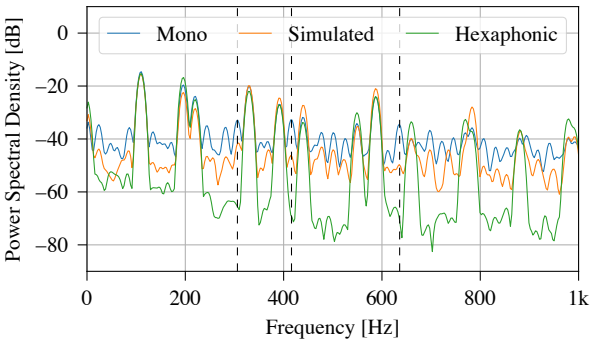

Figure 14: *Magnitude spectrum of each distortion output for the note pair* G_3–A_2. *The dashed lines show the three largest intermodulation components.*

begins with upsampling the mono input signal. A loop performs sample-based processing of each upsampled buffer. The parallel comb filter bank is implemented using twelve non-interpolating delay lines. Each individual signal is then distorted using the exponential distortion given in equation (22). Once distorted, the signals are mixed and downsampled to the original sampling frequency. Runtime measurements are summarized in Table 2. While the individual comb filtering operations are cheap, the cumulative cost of computing twelve parallel comb filters at sixteen times the sample rate quickly adds up. The upsampling and downsampling processes are comparatively cheap. The results also show that the implementation can in fact run in real-time, utilizing $1.324\,\mathrm{s}/8\,\mathrm{s} = 0.17$ real-time blocks.

Table 2: *Computational expense averaged over three runs. Clang optimization level -Os (fastest, smallest). Running on a 1.6 GHz Intel Core i5.*

8 s of 24-bit audio at 44.1 kHz, 16× oversampling

Process	Time [s]	Weight [%]
File Read	0.030	2.28
Upsample	0.042	3.14
Parallel Filters	$16 \times 12 \times 0.00311 = 0.598$	45.14
Distortion	$16 \times 12 \times 0.00265 = 0.510$	38.54
Mix	$16 \times 12 \times 0.00024 = 0.046$	3.47
Downsample	0.045	3.38
File Write	0.054	4.05
Total	1.324	100.00

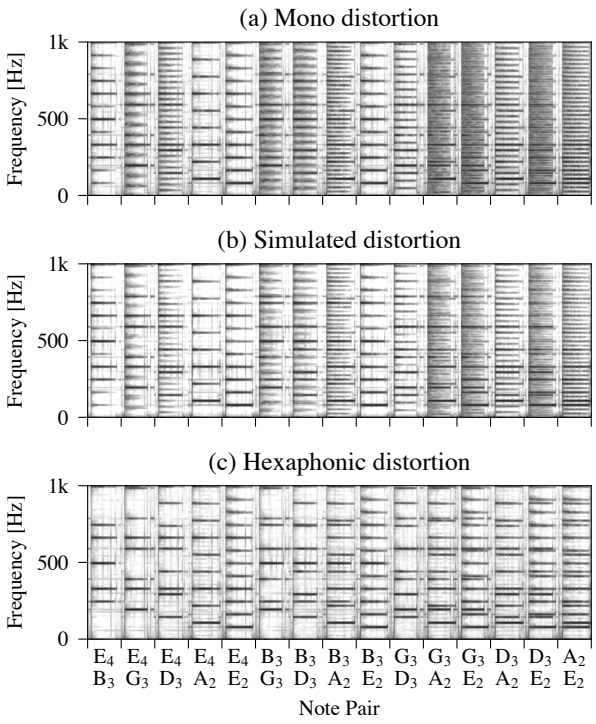

Figure 15: *Distortion spectrograms for pairwise combinations of open string notes.*

7. CONCLUSIONS

The simulated hexaphonic distortion effect described in this paper attempts to reproduce the characteristics of hexaphonic distortion for use with ordinary electric guitars with mono pickups. A parallel comb filter structure has been shown to separate a mono guitar signal into predominantly harmonic signals akin to that of a hexaphonic pickup signal. In addition, the overlapping spectral peaks of the comb filters simulate the sympathetic vibrations captured by hexaphonic pickups. Individually distorting the harmonically separated signals results in clear, sustained, and harmonically rich distortion with fewer intermodulation products. The algorithm therefore provides guitarists with greater flexibility in their choice of chords when using distortion. The proposed structure may be used in real-time with any sufficiently optimized distortion algorithm.

8. REFERENCES

[1] U. Zölzer, Ed., *DAFX: Digital Audio Effects*, pp. 70–79, 101–106, 126, John Wiley & Sons, 2nd edition, 2011.

[2] J. E. R. de Paiva, "Os Mutantes: Hibridismo tecnológico na música popular brasileira dos anos 60/70," *Revista Sonora*, vol. 4, no. 7, pp. 1–7, 2012.

[3] R. Dobson, *A Dictionary of Electronic and Computer Music Technology: Instruments, Terms, Techniques*, pp. 66, 89–91, 121, Oxford University Press, 1992.

[4] R. Graham and J. Harding, "SEPTAR: Audio breakout circuit for multichannel guitar," in *Proc. Int. Conf. New Interfaces for Musical Expression (NIME)*, Baton Rouge, LA, USA, May 31 – June 3 2015, pp. 241–244.

[5] C. Anderton, "Build the super-versatile Quadrafuzz: Four fuzzes in one with active EQ," *Guitar Player Mag.*, pp. 37–46, June 1984.

[6] P. Fernández-Cid and J. Casajús Quirós, "Distortion of musical signals by means of multiband waveshaping," *J. New Music Res.*, vol. 30, no. 3, pp. 219–287, 2001.

[7] J. Timoney, V. Lazzarini, A. Gibney, and J. Pekonen, "Digital emulation of distortion effects by wave and phase shaping methods," in *Proc. 13th Int. Conf. Digital Audio Effects (DAFx-10)*, Graz, Austria, Sept. 6–10 2010.

[8] J. S. Abel and K. J. Werner, "Distortion and pitch processing using a modal reverb architecture," in *Proc. 18th Int. Conf. Digital Audio Effects (DAFx-15)*, Trondheim, Norway, Nov. 30 – Dec. 3 2015.

[9] A. Novak, L. Guadagnin, B. Lihoreau, P. Lotton, E. Brasseur, and L. Simon, "Non-linear identification of an electric guitar pickup," in *Proc. 19th Int. Conf. Digital Audio Effects (DAFx-16)*, Brno, Czech Republic, Sept. 5–9 2016, pp. 241–246.

[10] G. Evangelista and M. Raspaud, "Simplified guitar bridge model for the displacement wave representation in digital waveguides," in *Proc. 12th Int. Conf. Digital Audio Effects (DAFx-09)*, Como, Italy, Sept. 1–4 2009.

[11] V. Välimäki, H.-M. Lehtonen, and T. I. Laakso, "Musical signal analysis using fractional-delay inverse comb filters," in *Proc. 10th Int. Conf. Digital Audio Effects (DAFx-07)*, Bordeaux, France, Sept. 10–15 2007, pp. 261–268.

[12] S. J. Orfanidis, *Introduction to Signal Processing*, pp. 202–210, 409–421, Prentice Hall, 2010.

[13] T. Miwa, Y. Tadokoro, and T. Saito, "Musical pitch estimation and discrimination of musical instruments using comb filters for transcription," in *Proc. 42nd Midwest Symp. Circuits and Syst.*, Las Cruces, NM, USA, Aug 8–11 1999, pp. 105–108.

[14] M. Gainza, R. Lawlor, and E. Coyle, "Harmonic sound source separation using FIR comb filters," in *Proc. 117th Audio Eng. Soc. Conv.*, San Francisco, CA, USA, Oct. 28–31 2004.

[15] J. Pekonen and V. Välimäki, "Filter-based alias reduction for digital classical waveform synthesis," in *Proc. IEEE Int. Conf. Acoust., Speech, and Signal Process. (ICASSP)*, Las Vegas, NV, USA, Mar. 2008, pp. 133–136.

[16] P. Rubenstein, "Ubertar Hexaphonic Guitar Pickups," Available at http://www.ubertar.com/hexaphonic/, accessed Dec. 30, 2019.

[17] M. R. Schroeder, "Natural sounding artificial reverberation," *J. Audio Eng. Soc.*, vol. 10, no. 3, pp. 219–223, 1962.

[18] A. Vaneev, "r8brain-free-src: High-quality pro audio sample rate converter / resampler C++ library," Available at https://github.com/avaneev/r8brain-free-src, 2019.

[19] S. Laguerre, "DAFx20-Hex-Sim: Audio files accompanying the DAFx 2020 paper," Available at https://slaguerre2.github.io/DAFx20-Hex-Sim/, 2020.

[20] P. R. Cook and G. P. Scavone, "The Synthesis ToolKit in C++ (STK)," Available at http://ccrma.stanford.edu/software/stk/, 2019.